Magnetostructural coupling and magnetocaloric effect in Ni-Mn-Ga-Cu microwires

Cite as: Appl. Phys. Lett. **108**, 052401 (2016); https://doi.org/10.1063/1.4941232
Submitted: 09 October 2015 • Accepted: 21 January 2016 • Published Online: 01 February 2016

Xuexi Zhang, Mingfang Qian, Zhe Zhang, et al.

Magnetostructural coupling and magnetocaloric effect in Ni-Mn-Ga-Cu microwires

Xuexi Zhang,[a] Mingfang Qian, Zhe Zhang, Longsha Wei, Lin Geng, and Jianfei Sun
School of Materials Science and Engineering, Harbin Institute of Technology, Harbin 150001, China

(Received 9 October 2015; accepted 21 January 2016; published online 1 February 2016)

Ni-Mn-Ga-X microwires were produced by melt-extraction technique on a large scale. Their shape memory effect, superelasticity, and damping capacity have been demonstrated. Here, the excellent magnetocaloric effect was revealed in Ni-Mn-Ga-Cu microwires produced by melt-extraction and subsequent annealing. The overlap of the martensitic and magnetic transformations, i.e., magnetostructural coupling, was achieved in the annealed microwires. The magnetostructural coupling and wide martensitic transformation temperature range contribute to a large magnetic entropy change of $-8.3\,\mathrm{J/kg\,K}$ with a wide working temperature interval of $\sim 13\,\mathrm{K}$ under a magnetic field of 50 kOe. Accordingly, a high refrigeration capacity of $\sim 78\,\mathrm{J/kg}$ was produced in the annealed microwires. [http://dx.doi.org/10.1063/1.4941232]

Magnetocaloric effect (MCE), a reversible temperature change under an applied magnetic field, shows superior application potential over conventional gas-vapor cycle because of its high efficiency, compactness, and environmental friendliness.[1] In Ni-Mn-based Heusler alloys,[2–8] the MCE may be produced in the vicinity of the first-order structural martensitic transformation (MT) and the second-order magnetic transformation. When the structural and magnetic transformations overlap, i.e., magnetostructural coupling takes place, giant magnetic entropy change (ΔS_m) may be obtained.[3,5,9] Ni-Mn-Ga alloys, which first attracted attention due to the giant magnetic-field-induced strain (MFIS),[10–12] can be tuned to reach a magnetostructural coupling state by changing their chemical compositions.[3] However, the magnetic transformation temperature (Curie point T_c) of Mn rich $Ni_{50}Mn_{25+x}Ga_{25-x}$ alloy varies little with composition in the vicinity of $e/a \approx 7.7$, where e/a represents the electron valence concentration.[13] As a result, the magnetostructural coupling and the corresponding giant ΔS_m can only occur around the nearly invariable T_c temperature. Besides, the magnetic entropy change associated with the first-order MT is normally concentrated in a relatively narrow temperature range.[3]

A fourth element doping in Ni-Mn-Ga alloys can change both martensitic and magnetic transformation temperatures, and may thus lead to a magnetostructural coupling around room temperature.[14] Among various doping elements, Cu element draws more attention because of its low cost, high efficiency in tuning the transformation temperatures, and enhancing the MCE.[14,15] For stoichiometric Ni_2MnGa alloy, its MT temperature is much lower than the magnetic transformation temperature. The MT temperature was increased, and the T_c was lowered after Cu substitution of Mn. Consequently, the occurrence of magnetostructural coupling, and thus the giant ΔS_m around room temperature, was achieved.[15–18] Cu substitution of Mn also increased the atomic ordering of Ni-Mn-Ga alloy, and thus favored the MCE.[19] As Ga is the most expensive element in Ni-Mn-Ga alloys, Cu substitution of Ga is cost-effective. In particular, Cu substitution of Ga increased the plasticity of Ni_2MnGa alloy when the Cu content is >18%.[20,21] At an intermediate Cu content of $8\% < x \leq 10\%$, a single phase alloy exhibiting excellent plasticity and a high temperature shape memory effect was achieved.[20,21] Furthermore, an increase in MT temperature and decrease in T_c was also confirmed at a low Cu content of $3\% < x \leq 4\%$.[22]

Compared to ternary Ni-Mn-Ga alloys, quaternary Ni-Mn-Ga-Cu alloys are ductile, cost-effective, and able to attain magnetostructural coupling at optimum compositions. Since Ni-Mn-Ga alloys are brittle and hard to shape at room temperature, the ways to improve their ductility are especially attractive.[20,21] The development of small size materials, such as particles, fibers, and films,[6,9,23–25] are possibly helpful. For example, small size components may be used as building blocks for complex devices, precursors for composite materials, and in micro-electromechanical systems.[26,27] Their high specific surface area promises a fast, efficient heat exchange, which is beneficial for magnetic cooling.[23] In our previous works,[28–30] Ni-Mn-Ga microwires were fabricated by the melt-extraction technique, and the shape memory effect and superelasticity properties have been demonstrated. Here, Ni-Mn-Ga-Cu microwires were fabricated by the melt-extraction method and then subjected to a chemical ordering annealing heat treatment. The annealed microwires exhibited large ΔS_m with wide working temperature interval, which was attributed to the magnetostructural coupling and wide MT temperature range.

Ni-Mn-Ga-Cu alloy parent ingot with a nominal composition of $Ni_{48.8}Mn_{26.7}Ga_{20.8}Cu_{3.7}$ (atomic percent) was prepared by induction melting pure Ni (99.99%), Mn (99.98%), Ga (99.99%), and Cu (99.99%) under argon atmosphere and casting in a copper mold. The ingot was re-melted four times to ensure the compositional homogeneity. The detailed process for microwire preparation by melt-extraction technique has been reported in Refs. 29 and 30. The as-extracted

[a]Author to whom correspondence should be addressed. Electronic mail: xxzhang@hit.edu.cn. Tel.: +86-451-86415894. Fax: +86-451-86413921.

microwires were sealed in a quartz ampoule, vacuumed, backfilled with 50 Pa pure Ar gas, and finally subjected to a stepwise chemical ordering annealing at 998 K/2 h, 973 K/10 h, and 773 K/20 h, followed by furnace cooling to room temperature. The compositions were determined by a Zeiss-SUPRA SEM equipped with an Oxford EDS using 20 kV voltage, 97 μA emission current, 10 mm work distance, 50 μA probe current, and >60 s data acquisition time duration. The composition measurement precision of the EDS was calibrated with chemical analysis results (ICP-OES) to be less than 0.5%. The MT temperatures were measured using a TA Q2000 differential scanning calorimeter (DSC) with cooling and heating rates of 5 K/min. The crystal structures of the parent ingot and microwires were determined in a Rigaku D/max-γA X-ray diffractometer with Cu Kα radiation ($\lambda = 1.54$ Å) at room temperature. The magnetization measurements were carried out using a vibrating sample magnetometer (VSM) in Physical Property Measurement System (PPMS) of Quantum Design, where the magnetic field was applied along the axis of the microwire in order to minimize the influence of the demagnetization field.

The melt-extraction technique is facile in preparing microwires with diameters of 20–80 μm and lengths of 30–150 mm on a large scale (Fig. S1).[31] During melt-extraction, the cooling rate of the extracted filaments may reach 10^4–10^5 K/s,[32] implying a grain refinement in the as-extracted microwires after solidification, as illustrated in Fig. 1(a). The cellular grains on the surface of the microwires have small diameters of 0.5–3 μm. In contrast, the grains on the surface of the annealed microwires become larger, with diameters of 1–15 μm, as shown in Fig. 1(b). Twins covering

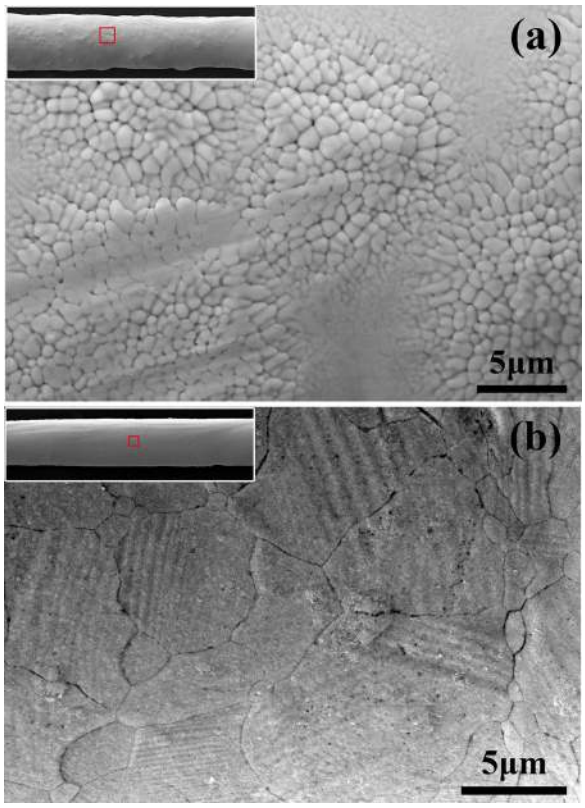

FIG. 1. SEM micrographs showing grains on the surface of (a) as-extracted and (b) annealed Ni-Mn-Ga-Cu microwires.

TABLE I. Compositions of the Ni-Mn-Ga-Cu parent ingot, as-extracted and annealed microwires.

	Composition (at. %)							
Materials	*Ni*	ΔNi	*Mn*	ΔMn	*Ga*	ΔGa	*Cu*	ΔCu
Parent ingot	49.3	0.1	26.3	0.1	20.8	0.1	3.6	0.1
As-extracted wires	49.4	0.3	26.2	0.2	20.7	0.3	3.7	0.1
Annealed wires	49.4	0.3	26.1	0.4	20.8	0.4	3.7	0.1

the width of the grains are also observed in Fig. 1(b), indicating a martensitic state of the annealed microwire at room temperature. The XRD patterns shown in Fig. S2[31] reveal that the parent ingot, the as-extracted and annealed microwires are in a single-phase seven layered modulated (7M) martensite state at room temperature. By the whole pattern fitting analysis, the 7M martensite was determined to be a monoclinic incommensurate superstructure[33] with lattice constants $a = 4.28$ Å, $b = 5.49$ Å, $c = 42.23$ Å, and $\beta = 92.5°$ for the ingot, $a = 4.25$ Å, $b = 5.52$ Å, $c = 42.22$ Å, and $\beta = 93.3°$ for the as-extracted microwire, and $a = 4.25$ Å, $b = 5.52$ Å, $c = 42.10$ Å, and $\beta = 93.5°$ for the annealed microwires, respectively.

The compositions of the parent ingot, as-extracted and annealed microwires are summarized in Table I. Compared to the nominal composition, the Mn loss contents caused by evaporation during melting, melt-extraction, and annealing are 0.4%, 0.5%, and 0.6%, respectively. The standard deviations of Ni, Mn, and Ga (ΔNi, ΔMn, and ΔGa) are higher in the microwires than those of the parent ingot, showing that the composition is less homogeneous in the microwires. As the MT temperatures of Ni-Mn-based Heusler alloys are strongly dependent on the composition,[13] the increased MT temperature range (i.e., $A_f - A_s$ and $M_s - M_f$) attributed to the composition deviation is expected.

Fig. 2 reveals the DSC curves of the parent ingot and the microwires. The microwires exhibit lower MT temperatures than the parent ingot. In addition, the MT temperatures of the as-extracted Ni-Mn-Ga-Cu microwires increase after annealing, which is consistent with Ni-Mn-Ga microwires.[28] The detailed transformation temperatures, M_s, M_f, A_s, A_f, and T_c, are summarized in Table II. The A_s of the parent ingot,

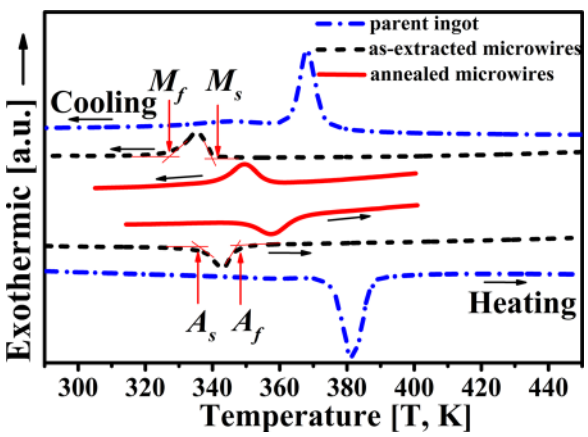

FIG. 2. DSC heating and cooling curves of the Ni-Mn-Ga-Cu parent ingot, as-extracted and annealed microwires.

TABLE II. Martensitic and magnetic transformation temperatures of the Ni-Mn-Ga-Cu parent ingot and microwires from DSC and low field *M-T* curves.

	Transformation temperatures (K)							
Materials	A_s	A_f	M_s	M_f	T_c	A_f-A_s	M_s-M_f	Hysteresis
Parent ingot	376.5	387.4	373.0	363.6	348.3	10.9	9.4	13.2
As-extracted wires	338.0	347.3	340.0	328.8	337.1	9.3	11.2	8.2
Annealed wires	350.6	365.4	356.4	342.8	356.0	14.8	13.6	8.1

as-extracted and annealed microwires are 376.5, 338.0, and 350.6 K, respectively. The transformation temperature ranges $A_f - A_s$ and $M_s - M_f$ of the annealed microwires are 14.8 and 13.6 K, respectively; both are larger than those of the parent ingot and the as-extracted microwire. The transformation hystereses, defined as the difference of DSC peaks during heating/cooling, are also presented in Table II. The as-extracted and annealed microwires exhibit smaller transformation hysteresis compared with the parent ingot, which is probably due to the smaller constraints caused by grain boundaries. Supposing that a microwire has a diameter of 50 μm and a length of 50 mm, the specific surface area (surface-to-volume ratio) of the microwire is ~6.2 times larger than that of the cubic bulk alloy. Therefore, the larger surface areas and fewer constraints may lead to the smaller thermal hysteresis in the microwires.

Chemical ordering annealing can increase the long range atomic ordering and reduce the defect density and internal stress, and thus may increase the saturation magnetization of the alloys.[28,34–36] According to the Maxwell relation, a higher value of $\partial M/\partial T$ implies a higher MCE. Therefore, larger magnetization difference ΔM is required for the enhancement of MCE. Fig. 3(a) displays the thermo-magnetization curves (*M-T*) of the annealed microwire under 0.2 kOe. Compared with the as-extracted microwire (Fig. S3), the magnetization property of the annealed one was significantly improved.[31] A small thermal hysteresis of ~4 K is obtained during heating and cooling. The abrupt changes of magnetization occur at temperatures within 345–365 K. The inset in Fig. 3(a) is a first derivative plot of the field heating (FC) curve. A peak centered at 356 K is observed, which corresponds to the magnetic transition temperature T_c. In order to further confirm the T_c, the so-called Arrott plots, M^2 vs H/M plots, were derived from the isothermal magnetic *M-H* curves, as shown in Fig. 3(b). The intersection of the vertical axis is positive at 356 K but negative at 358 K, indicating that T_c falls within the range of 356–358 K, which confirmed the T_c temperature.[37] In particular, DSC curves in Fig. 3(a) show that M_f^{DSC} occur inside the ferromagnetic region while A_f^{DSC} inside the paramagnetic region. So, the overlap of the structural and magnetic transformations takes place, meaning that the ferromagnetic martensite directly transformed to paramagnetic austenite during heating process. Due to the magnetostructural coupling, the distance between the magnetic atoms (such as Mn–Mn) in crystal lattices changes, attributed to the spontaneous structural transition, accompanying with the magnetic transition, which enlarges the ΔM. Considering the magnetostructural coupling and the wide MT temperature range in the annealed

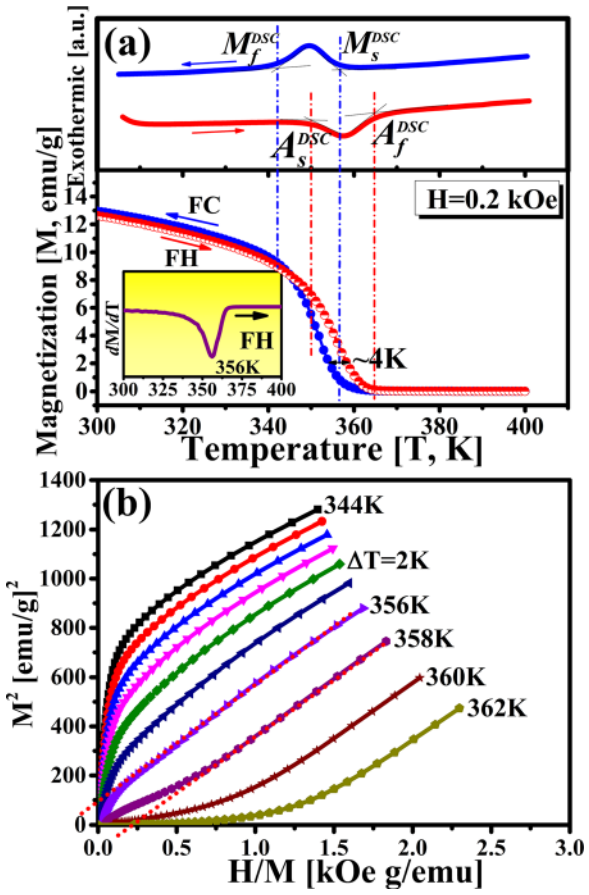

FIG. 3. (a) Heating and cooling DSC curves (upper) and *M-T* curves at 0.2 kOe (lower). The inset in (a) shows the first derivation of the field heating FH plot in which the peak temperature 356.0 K were defined as the Curie point T_c; (b) M^2 vs H/M plots (Arrott plots) of the annealed Ni-Mn-Ga-Cu microwire derived from the isothermal magnetization data within temperatures 344–362 K.

microwire, a large magnetic entropy change and a wide working temperature interval are expected.

The magnetic entropy change ΔS_m was calculated from the magnetic isotherms (as shown in Fig. 4(a)) using the Maxwell relation: $\Delta S_m(T,H)_{\Delta H} = \int_0^{H_{\max}} (\frac{\partial M}{\partial T})_H dH$. From the numerical integration of $\partial M/\partial T$ from *M-H* curves at various applied field, the magnetic entropy change ΔS_m was obtained, as displayed in Fig. 4(b). The maximum $\Delta S_m - 8.3$ J/kg K was found at 359 K under 50 kOe, which is much higher than those of the Ni-Mn-In-Co[38] and Ni-Mn-Ga-Fe[39] microwires. The field dependence of the maximum ΔS_m shown in the inset of Fig. 4(b) exhibits nearly linear magnetic field dependence and ΔS_m does not saturate under the magnetic field of 50 kOe.

From Fig. 4(b), a large full width at half maximum (FWHM) of ~13 K can be attained. Here, the refrigeration capacity (RC), which is a measure of the adiabatic heat produced between the cold (T_1) and hot (T_2) reservoirs in an ideal refrigeration cycle, was calculated by integrating the $\Delta S_m(T)$ curve over the FWHM: $RC = \int_{T_1}^{T_2} \Delta S_m(T)_H dT$. The field-dependence of RC is plotted in Fig. 4(c). A maximum RC is determined to be 78 J/kg under 50 kOe. Similar to ΔS_m (inset of Fig. 4(b)), the RC does not saturate under 50 kOe.

The maximum ΔS_m, FWHM, and RC of the present Ni-Mn-Ga-Cu microwire and other giant MCE alloys under 20

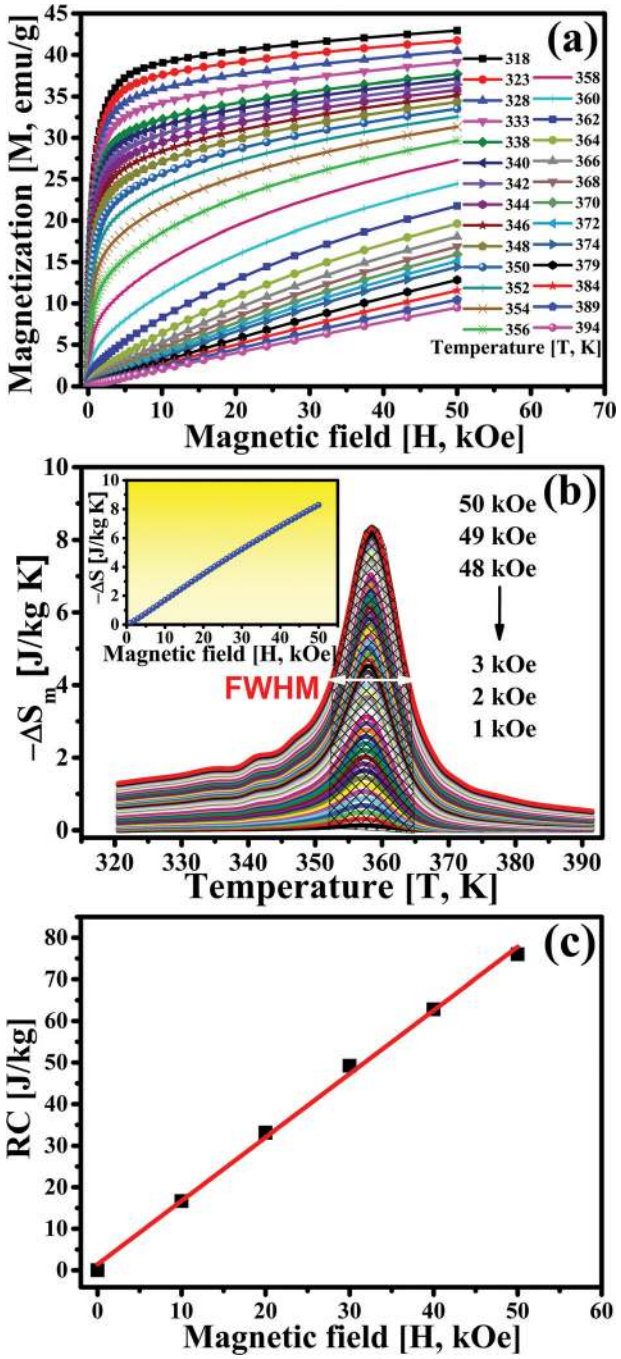

FIG. 4. (a) Isothermal magnetization *M-H* curves. (b) Temperature dependence of magnetic entropy change ΔS_m-T. The white double sided arrows show the FWHM under 50 kOe. The inset in (b) demonstrates the field dependence of absolute maximum magnetic entropy change $|\Delta S_m|$. (c) Field dependence of the refrigeration capacity (RC) in the annealed Ni-Mn-Ga-Cu microwires. The line in (c) only acts as a guide for the eye.

and 50 kOe are summarized in Table SI.[31] Under 50 kOe, the ΔS_m of the present Ni-Mn-Ga-Cu microwire (−8.3 J/kg K) is lower than the other alloys, but the FWHM of the Ni-Mn-Ga-Cu microwires (∼13 K) is larger than those of other Ni-Mn-based ribbons (R) or bulk (B) alloys (0.9–6.5 K).[3,9,14,17,19,40,41] The obtained RC in Ni-Mn-Ga-Cu microwire (78.0 J/kg) is comparable with those of Ni-Mn-based alloys (70–115 J/kg)[3,9,40] and superior to those of Ni-Mn-Ga-Cu bulk alloys (72–75 J/kg).[14,17,19] On the other hand, when compared to Gd[42] or $LaFe_{13-x}Si_x$[43] alloys, the Ni-Mn-Ga-Cu microwires are rare-earth free and thus cost effective, which helps for the practical applications.

Considering that high heat exchange efficiency is necessary for a magnetic refrigeration cycle, the microwires show advantages over bulk alloys because of their huge specific surface area. When a bundle of microwires was assembled into a porous compact, the gas or fluid flowing in and out of the pores may significantly enhance the heat exchange capacity between the magnetic refrigerants and heat exchange agents. By this strategy, complex shaped, high efficient and low cost magnetic refrigerant devices may be developed. The microwires may also act as building blocks for minor- and macro-devices, depending on the application requirements.

In conclusion, the $Ni_{49.4}Mn_{26.1}Ga_{20.8}Cu_{3.7}$ microwires were prepared by melt-extraction and subsequent chemical ordering annealing. A magnetostructural coupling state was created in the microwire after annealing. The annealed microwire also exhibited a wide MT temperature range. Consequently, a maximum ΔS_m of −8.3 J/kg K, FWHM of ∼13 K, and RC of ∼78 J/kg were obtained under 50 kOe. So, the annealed $Ni_{49.4}Mn_{26.1}Ga_{20.8}Cu_{3.7}$ microwire shows application potential as a kind of magnetic refrigeration material.

X.X.Z., M.F.Q., and L.G. are thankful to the financial support from National Natural Science Foundation of China (NSFC) (Grant No. 51001038). X.X.Z. and M.F.Q. also thank the financial support from the Ministry of Science and Technology Bureau of Harbin (Grant No. 2011RFQXG001).

[1]V. K. Pecharsky and K. A. Gschneidner, Phys. Rev. Lett. **78**, 4494 (1997).
[2]A. A. Cherechukin, T. Takagi, M. Matsumoto, and V. D. Buchel'Nikov, Phys. Lett. A **326**, 146 (2004).
[3]M. Pasquale, C. P. Sasso, L. H. Lewis, L. Giudici, T. Lograsso, and D. Schlagel, Phys. Rev. B **72**, 094435 (2005).
[4]T. Krenke, E. Duman, M. Acet, E. F. Wassermann, X. Moya, L. Manosa, and A. Planes, Nat. Mater. **4**, 450 (2005).
[5]M. Khan, S. Stadler, and N. Ali, J. Appl. Phys. **101**, 09C515 (2007).
[6]B. Hernando, J. L. S. Llamazares, J. D. Santos, V. M. Prida, D. Baldomir, D. Serantes, R. Varga, and J. Gonzalez, Appl. Phys. Lett. **92**, 132507 (2008).
[7]A. Planes, L. Manosa, and M. Acet, J. Phys.: Condens. Matter **21**, 233201 (2009).
[8]J. Liu, T. Gottschall, K. P. Skokov, J. D. Moore, and O. Gutfleisch, Nat. Mater. **11**, 620 (2012).
[9]Z. Li, Y. Zhang, C. F. Sánchez-Valdés, J. L. Sánchez Llamazares, C. Esling, X. Zhao, and L. Zuo, Appl. Phys. Lett. **104**, 44101 (2014).
[10]K. Ullakko, J. K. Huang, C. Kantner, R. C. O' Handley, and V. V. Kokorin, Appl. Phys. Lett. **69**, 1966 (1996).
[11]S. J. Murray, M. Marioni, S. M. Allen, R. C. O'Handley, and T. A. Lograsso, Appl. Phys. Lett. **77**, 886 (2000).
[12]A. Sozinov, A. A. Likhachev, N. Lanska, K. Ullakko, and V. K. Lindroos, J. Phys. IV **112**, 955 (2003).
[13]X. Zhou, H. Kunkel, G. Williams, S. Zhang, and X. Desheng, J. Magn. Magn. Mater. **372**, 305 (2006).
[14]S. Stadler, M. Khan, J. Mitchell, N. Ali, A. M. Gomes, I. Dubenko, A. Y. Takeuchi, and A. P. Guimarães, Appl. Phys. Lett. **88**, 192511 (2006).
[15]C. S. Mejiá, A. M. Gomes, and L. A. S. de Oliveira, J. Appl. Phys. **111**, 07A923 (2012).
[16]A. M. Gomes, M. Khan, S. Stadler, N. Ali, I. Dubenko, A. Y. Takeuchi, and A. P. Guimarães, J. Appl. Phys. **99**, 08Q106 (2006).
[17]J. F. Duan, Y. Long, B. Bao, H. Zhang, R. C. Ye, Y. Q. Chang, F. R. Wan, and G. H. Wu, J. Appl. Phys. **103**, 063911 (2008).
[18]S. Roy, E. Blackburn, S. M. Valvidares, M. R. Fitzsimmons, S. C. Vogel, M. Khan, I. Dubenko, S. Stadler, N. Ali, S. K. Sinha, and J. B. Kortright, Phys. Rev. B **79**, 235127 (2009).

[19]C. Huang, Y. Wang, Z. Tang, X. Liao, S. Yang, and X. Song, J. Alloys Compd. **630**, 244 (2015).
[20]J. Wang, H. Bai, C. Jiang, Y. Li, and H. Xu, Mater. Sci. Eng. A **527**, 1975 (2010).
[21]P. P. Li, J. M. Wang, and C. B. Jiang, J. Phys. D: Appl. Phys. **44**, 285002 (2011).
[22]I. Glavatskyy, N. Glavatska, A. Dobrinsky, J. U. Hoffmann, O. Söderberg, and S. P. Hannula, Scr. Mater. **56**, 565 (2007).
[23]R. Niemann, O. Heczko, L. Schultz, and S. Fähler, Appl. Phys. Lett. **97**, 222507 (2010).
[24]N. S. Bingham, H. Wang, F. Qin, H. X. Peng, J. F. Sun, V. Franco, H. Srikanth, and M. H. Phan, Appl. Phys. Lett. **101**, 102407 (2012).
[25]F. X. Qin, N. S. Bingham, H. Wang, H. X. Peng, J. F. Sun, V. Franco, S. C. Yu, H. Srikanth, and M. H. Phan, Acta Mater. **61**, 1284 (2013).
[26]N. Scheerbaum, D. Hinz, O. Gutfleisch, K. H. Müller, and L. Schultz, Acta Mater. **55**, 2707 (2007).
[27]S. Glock, X. X. Zhang, N. J. Kucza, P. Müllner, and V. Michaud, Composites, Part A **63**, 68 (2014).
[28]M. F. Qian, X. X. Zhang, L. S. Wei, L. Geng, and H. X. Peng, J. Alloys Compd. **645**, 335 (2015).
[29]M. F. Qian, X. X. Zhang, C. Witherspoon, J. F. Sun, and P. Müllner, J. Alloys Compd. **577**, S296 (2013).
[30]M. F. Qian, X. X. Zhang, L. S. Wei, P. G. Martin, J. F. Sun, L. Geng, T. B. Scott, L. V. Panina, and H. X. Peng, J. Alloys Compd. **660**, 244–251 (2015).
[31]See supplementary material at http://dx.doi.org/10.1063/1.4941232 for the information for the macro-morphology of the melt-extracted $Ni_{49.4}Mn_{26.2}Ga_{20.7}Cu_{3.7}$ microwires (Fig. S1), which exhibit a diameter of 20–80 μm and a length of 30–150 mm, and the X-ray diffraction patterns of the parent ingot, as-extracted and annealed microwires (Fig. S2) showing that they contain seven-layer modulated (7M) martensite phase with a monoclinic incommensurate superstructure. The DSC and *M-T* curves (Fig. S3) show that the magnetostructural coupling occurs in the as-extracted microwires as well, and that the magnetization is much lower compared with the annealed microwires measured at the same field strength (see Fig. 3(a)). The maximum entropy change ΔS_m, full width at half maximum (FWHM), and refrigeration capacity RC of the annealed Ni-Mn-Ga-Cu microwire and some other giant MCE alloys are summarized in Table SI.
[32]G. Lotze, G. Stephani, W. Loser, and H. Fiedler, Mater. Sci. Eng. A **133**, 680 (1991).
[33]L. Righi, F. Albertini, E. Villa, A. Paoluzi, G. Calestani, V. Chernenko, S. Besseghini, C. Ritter, and F. Passaretti, Acta Mater. **56**, 4529 (2008).
[34]O. Heczko, P. Svec, D. Janickovic, and K. Ullakko, IEEE Trans. Magn. **38**, 2841 (2002).
[35]F. Albertini, S. Besseghini, A. Paoluzi, L. Pareti, M. Pasquale, F. Passaretti, C. P. Sasso, A. Stantero, and E. Villa, J. Magn. Magn. Mater. **242**, 1421 (2002).
[36]J. Gutierrez, J. M. Barandiaran, P. Lazpita, C. Segui, and E. Cesari, Sens. Actuators, A **129**, 163 (2006).
[37]Y. Zhang, R. A. Hughes, J. F. Britten, P. A. Dube, J. S. Preston, G. A. Botton, and M. Niewczas, J. Appl. Phys. **110**, 013910 (2011).
[38]X. X. Zhang, S. P. Miao, and J. F. Sun, Trans. Nonferrous Met. Soc. China **24**, 3152 (2014).
[39]Y. F. Liu, X. X. Zhang, D. W. Xing, H. X. Shen, D. M. Chen, J. S. Liu, and J. F. Sun, J. Alloys Compd. **616**, 184 (2014).
[40]S. K. Srivastava, V. K. Srivastava, and R. Chatterjee, Solid State Commun. **152**, 372 (2012).
[41]Y. Zhang, L. L. Zheng, Q. Zheng, X. Q. Li, M. Li, J. Du, and A. Yan, Sci. Rep. **5**, 11010 (2015).
[42]S. Y. Dan'Kov, A. M. Tishin, V. K. Pecharsky, and K. A. Gschneidner, Jr., Phys. Rev. B **57**, 3478 (1998).
[43]O. Gutfleisch, A. Yan, and K. H. Müller, J. Appl. Phys. **97**, 10M305 (2005).